ELSEVIER

Journal of Molecular Catalysis A: Chemical 100 (1995) 75–85

JOURNAL OF MOLECULAR CATALYSIS A: CHEMICAL

A quantum-chemical study of *para*/*ortho*-toluene alkylation by adsorbed methoxy species on zeolites

A. Corma [a,*], G. Sastre [a], P.M. Viruela [b]

[a] *Instituto de Technologia Quimica UPV-CSIC Universidad Politecnica de Valencia, Avenida de los Naranjos s/n, 46071 Valencia, Spain*

[b] *Departamento de Quimica Fisica, Universidad de Valencia, Doctor Moliner, 50, 46100 Burjassot (Valencia), Spain*

Received 1 June 1995

Abstract

MNDO and PM3 semiempirical methods have been employed to study the mechanism of toluene alkylation by methanol on zeolites, by means of the cluster $(H)_3SiO(CH_3)T(H)_2OSi(H)_3$ in were T = Al, B, Ga. Two possible reaction mechanisms have been found. The first one corresponds to the classical process of aromatic electrophilic substitution, in which the transition state of the reaction shows distances and angles according to the precursor of the Wheland intermediate. The second mechanism proceeds in one concerted step, in which the transfer of the proton from the toluene to the basic oxygen of the zeolite is simultaneous to the transfer of the methyl cation from the zeolite to the toluene. The effect of chemical composition of the cluster on regioselectivity has been studied, and perturbed molecular orbital (PMO) analysis of the system at the ab initio HF/STO-3G level has shown that covalent interactions are important. The energy of the covalent interaction between the molecular orbitals of the toluene and the cluster mainly HOMO–LUMO, are more important in *para* than in *ortho* positions.

Keywords: Alkylation; Methoxy species; Toluene; Zeolites

1. Introduction

Acid strength is one of the most important factors controlling reactivity and selectivity of zeolites catalyst for carboniogenic reactions [1,2]. In order to predict zeolite acidity, properties like geometry, chemical composition, charge distribution, electronegativity, and vibration frequencies have been correlated with acid strength [3–5]. Thus, reactions are classified from the point of view of the acid strength needed to form the initial carbocation. In this way, it is believed that the alkylation of toluene by alcohols requires sites of medium–strong acidity [6]. Owing to the commercial importance of the products obtained, i.e. xylenes and ethyl toluene, it is not surprising that a large effort has been devoted to optimize the acid strength distribution and geometry of alkylation catalysts [7]. From the point of view of the reaction mechanism, the existence of available tools for carrying out the adsorption of reactants in infrared cells, has contributed to the identification of possible alkylating species [8]. In this way, it has been shown that at low temperatures, methoxonium and methoxy species can coexist. However, when the temperature increases, the equilibrium is shifted toward methoxy species [9], and these or, even better, activated methoxy species are believed to be the alkylating agents

* Corresponding author. Tel. (+34-6)3877800, fax (+34-6)3877809.

SSDI 1381-1169(95)00129-8

during the electrophilic alkylation of aromatics by methanol [10]. While the first step of the reaction i.e. alcohol adsorption, is relatively well established, the alkylation reaction itself is difficult to follow experimentally, and the detailed mechanism is still unknown.

The aim of this work is to study by semiempirical quantum-chemistry the mechanism of toluene alkylation by alcohols on zeolites. In this way the intermediate species, and transition states have been found and characterized, and the influence of zeolite composition on the reaction path and energetic of the process have been studied. Finally, the role of the covalent interactions in the electrophilic aromatic substitution catalyzed by zeolites have been established by performing perturbed molecular orbital (PMO) analysis in the transition state of the first mechanism found, showing in a semi-quantitative calculation the HOMO–LUMO interactions between the toluene and the catalyst. This allowed us to discuss the possibilities for finding regioselectivity in the case of large pore zeolites in where shape selective effects can not be claimed.

2. Methodology

In this work, we have carried out a detailed study of the reaction pathway for the alkylation of toluene by methanol on zeolite clusters using molecular orbital calculations. The differences in *para* and *ortho* alkylation, the activation enthalpy of the process and its possible variation when changing the chemical composition of the clusters has been studied by means of PM3 (modified neglect of differential overlap parametrization method 3) [11] and MNDO (modified neglect of differential overlap) [12] quantum-chemical semiempirical methods.

The calculations were done with the system package MOPAC 6.0 [13] and run with a IBM 9021/500-2VF computer. The structure of reactants and products was localized by using the BFGS (Broyden, Fletcher, Goldfarb, and Shanno) optimization method [14]. In most of the cases a first approximation to the transition state structure was obtained by analysis of potential hypersurfaces obtained by scanning the more important parameters of the reaction. The transition states were localized with the TS subroutine which searches the points of the hypersurface with only one negative value of the hessian matrix [15]. Once these points were localized, their characterization was done by the FORCE subroutine, which diagonalizes the hessian matrix and calculates the normal vibration modes.

The methods MNDO and PM3 give good geometries, and have been largely used with success [16]. Nevertheless, it has to be considered that in the case of the transition states, the absolute values of activation energies calculated with these methods are not expected to be realistic [17], and they should only be used on a comparative bases for a series of calculations.

The zeolite cluster used in the calculations to simulate the alkylating complex is the simplest necessary for the reaction of toluene alkylation to occur, and contains two active centers: one acidic and one basic. The small size of this cluster is very useful to carry out the large amount of calculations involved when considering several parameters along a reaction hypersurface. In the calculations the zeolite skeleton (Si–O–T–O–Si) was kept fixed in a plane, and the terminal hydrogens were symmetrically placed with respect to this plane. Those restrictions serve to simulate the relative rigidity of a real zeolite. The MNDO calculations included the substitutions T = B and Al; and the PM3 included T = Al and Ga.

The results of this work must be related with alkylation processes on large pore zeolites in where there are not stearic constraints.

The transition state geometry obtained in the first mechanism found, served to show the role of the covalent interactions between the toluene and the alkylating agent. This was demonstrated by carrying out perturbed molecular orbital (PMO) analysis with the fixed geometry of the transition state of HF/STO-3G [18] level and using the MONSTERGAUSS package [19].

3. Results and discussion

As it was said above, in the first step of the reaction there is an attack of methanol to the acid center of the zeolite, and as a result the alkylating agent is obtained [20]. Several alkylating agents have been proposed in the literature [21], but in this case, the methoxonium and methoxy species are the most stables. The equilibrium among is displaced to the methoxy species when the temperature increases above 200°C. Once formed, the alkylating agent will react with a molecule of toluene and the result will be the final products of the reaction, i.e., the xylenes. The scheme of the two steps of the reaction is as follows (T = B, Al, Ga):

step 1: $CH_3OH + -SiO(H)ToSi- \rightarrow -SiO(CH_3)TSi- + H_2O$

step 2: $-SiO(CH_3)TOSi- + Ph-CH_3 \rightarrow -SiO(H)TOSi- + Ph-(CH_3)_2$

In this work we have started with the alkylating agent already formed [21], and this has been considered to be a methoxide cluster of zeolite. The optimized geometries for these clusters (Fig. 1) are similar to those obtained from calculations performed with the Hartree–Fock/3-21G ab initio method [22]. In our results the values obtained with the two methods are of the same order, and the most relevant differences were found in the

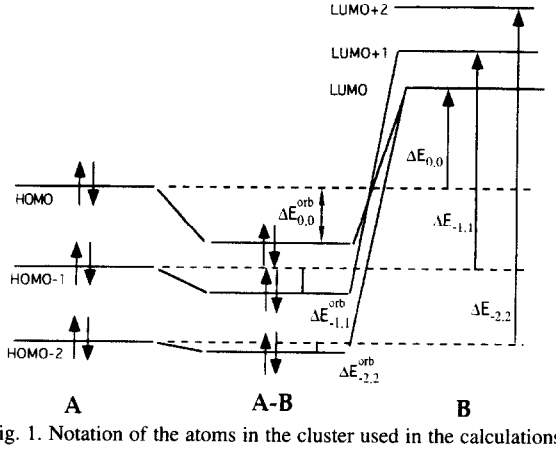

Fig. 1. Notation of the atoms in the cluster used in the calculations and parameters of the reaction coordinate. T = B, Al, Ga.

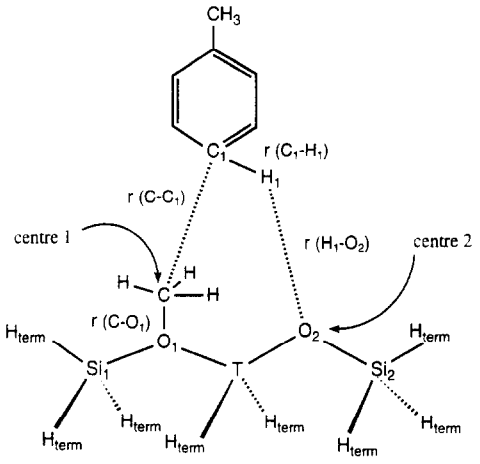

Fig. 2. More important geometrical parameters optimized for the zeolite–CH_3 cluster. (a) PM3 calculations. (b) MNDO calculations.

Si_1O_1T and TO_2Si_2 angles. The O_1TfO_2 angles obtained are tetrahedral. In the PM3 calculations, the values 137.8° and 132.4° were obtained for the Si_1O_1Al and Si_1O_1Ga angles, respectively. In the MNDO case the results were 124.5° and 122.0° for the Si_1O_1 and Si_1O_1Al angles, respectively. Therefore, the angles obtained by using MNDO are smaller than for the PM3 method. The AlO_2Si_2 and GaO_2Si_2 angles are 152.7° and 178.0° respectively in PM3. In the MNDO the angles BO_2Si_2 and AlO_2Si_2 have the respective values of 134.2° and 166.6°. All these values are within the experimental range of zeolites [23]. The geometries obtained for the isolated cluster in the products zone are very similar to those presented above since the only difference between the clusters is the substituted group, i.e., CH_3 in reactants and H in products.

The reaction was studied through the evolution of toluene towards the zeolite and its subsequent alkylation, passing through the transition state. In order to simulate this complex interaction, a prospecting of the hypersurface of the reaction was done. The controlled parameters (Fig. 2) in the scanning were those considered as the most important in the evolution of reactants to products along the reaction pathway: the distances of methyl group to the cluster of the zeolite and to toluene, $r(C–C_1)$ and $r(C–O_1)$ respectively; and the distances of the hydrogen atom of the toluene, H_1, to the cluster of the zeolite and to the toluene:

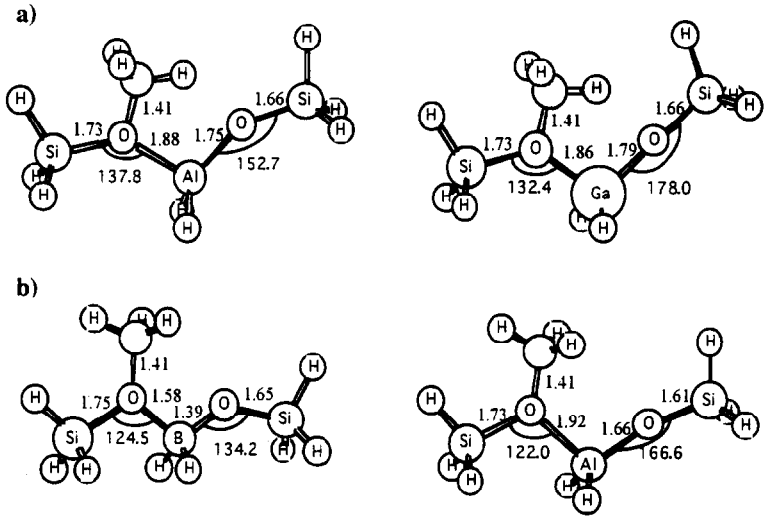

Fig. 3. Schematic representation of the structure for localized intermediates and transition states on different mechanisms of the para alkylation.

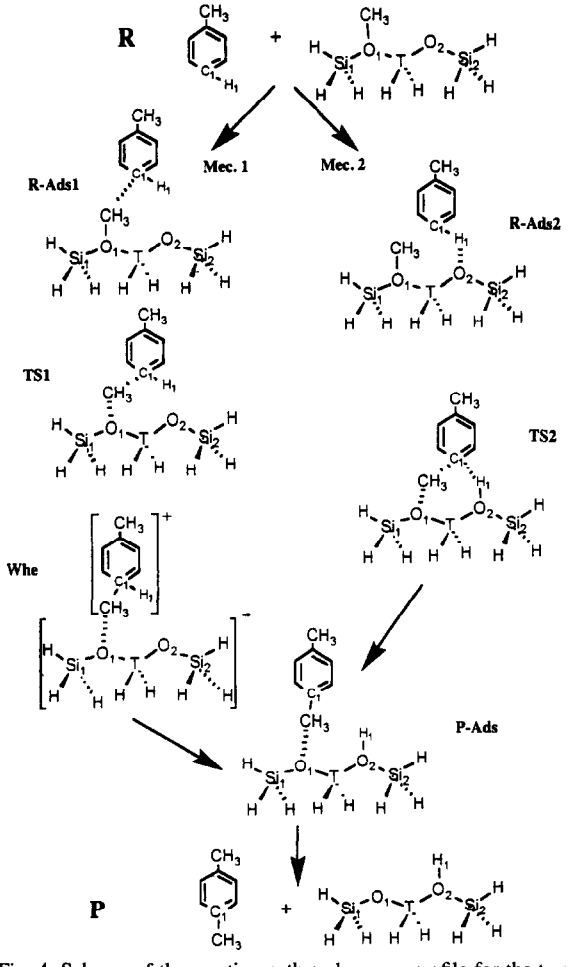

Fig. 4. Scheme of the reaction path and energy profile for the two mechanisms of the reaction.

$r(C_1–H_1)$ and $r(H_1–O_2)$. The scanning started in the reactants zone: $r(C–C_1) = 3.0$ Å, $r(C–O_1) = 1.4$ Å, $r(C_1–H_1) = 1.1$ Å, $r(H_1–O_2) = 4.0$ Å; and was followed until reaching the products zone: $r(C–C_1) = 1.5$ Å, $r(C–O_1) = 4.3$ Å, $r(C_1–H_1) = 4.1$ Å, $r(H_1–O_2) = 1.0$ Å. The parameters $r(C–C_1)$, $r(C–O_1)$, and $r(C_1–H_1)$ were varied smoothly in intervals of 0.1 Å, and were controlled simultaneously in order to prevent discontinuities in the energy hypersurface. In the prospecting, two reaction paths were found, which means that the reaction can occur, at least, through two different mechanisms. Then, if the $r(C–C_1)$, $r(C–O_1)$, and $r(C_1–H_1)$ variables are controlled starting with $r(H_1–O_2) \approx 1.8$ Å, one transition state is obtained. On the other hand, if the $r(C–C_1)$, $r(C–O_1)$, and $r(C_1–H_1)$ variables are controlled starting with $r(H_1–O_2) \approx 2.5$ Å, the second transition state is obtained. The difference between the two transition states, Fig. 3 and Fig. 4, is due to the interaction site of the toluene respect to the zeolite cluster. In the first case, *Mechanism* 1, the interaction site of toluene is one of the carbon atoms of the aromatic ring (C_1), which interacts with the CH_1 of the zeolitic counterpart. In the second case, *Mechanism* 2, the toluene forms a hydrogen bridged bond (H_1) with the basic center (O_2) of the cluster. The two mechanisms will be explained in more detail in the following section.

4. Reaction mechanisms

4.1. Mechanism 1

The *first step* of the reaction is an approach of toluene to the alkylating agent. In this case, the process corresponds to a physisorption, and the interaction takes place, as has been said above, between a carbon atom (C_1) of the toluene and the CH_3 group of the cluster. The enthalpy and position of the adsorbed complex is obtained by scanning the distance C–C_1. This calculation gives the geometry of the different adsorbed complexes (R_{ads1} in Table 1 and Table 2), and their adsorption energies (ΔH_{ads1} in Table 3). The geometries for the interaction in *ortho* and *para* positions are the same, and for this reason, only the *para*-geometries are showed. The results of the adsorption energies should not be considered in a quantitative sense because semiempirical methods calculate with low precision the long range interactions. The calculated enthalpies give only an approximation to the nature of the adsorption process and they indicate that there is a small influence of the chemical composition of the cluster and the position of interaction of toluene. Ab initio calculations carried out at SCF level using 3-21G basis set gave similar results [22].

This first mechanism corresponds to the classical electrophilic aromatic substitution in two steps. We can see that the toluene alkylation follows the adsorption step and, in our calculations, this is the rate determining step. The transition state obtained, TS1 (Fig. 3 and Fig. 4), has a geometry (Table 1 and Table 2) in which the methyl group is being transferred to the aromatic ring, forming a bond with the C_1. Meanwhile the hydrogen bonded to this carbon (H_1) remains at the equilibrium distance. With regards to selectivity, the activation energies (ΔH_{act1} in Table 3) in the *ortho* and *para* positions are almost the same, regardless of the chemical substitution (T^{III} = Al, B, Ga) in the cluster, and little differences in selectivity may be expected according to those results. However, it has to be considered that the high activation energies found in our calculations, owing to factors others than the reaction itself could hardly distinguish differences in the order of 3–5 kcal/mol which could, in principle, be large enough to explain the relatively small changes in the *para*/*ortho* selectivities observed experimentally on large pore zeolites [24]. Furthermore, it should be considered that when orbital

Table 1
Relevant geometric parameters obtained for reactants, transition states, Wheland complex and products using PM3 semiempirical method. The geometries correspond to *para* interaction. See Fig. 2 for labelling of geometrical parameters, and Fig. 5 for labelling of the species

Parameter	R_{adr1}		R_{adr1}		TS1		TS2		Whe		P_{ads}	
T=	Al	Ga	Al	Ga	Al	Ga	Al	Ga	Al	Ga	Al	Ga
$r(C–O_1)$	1.413	1.404	1.412	1.402	2.072	2.028	1.754	1.724	2.762	2.659	5.204	2.904
$r(C–C_1)$	3.748	4.224	5.903	3.746	1.993	1.962	2.123	2.102	1.544	1.518	1.493	1.492
$r(C_1–H_1$	1.102	1.112	1.118	1.123	1.217	1.223	4.152	4.934	1.114	1.134	–	–
$r(H_1–O_2)$	5.319	5.402	1.828	1.768	1.673	1.619	1.034	0.993	3.182	3.181	0.962	0.954
$r(Si_1–O_1)$	1.734	1.708	1.732	1.724	1.676	1.659	1.693	1.679	1.654	1.713	1.673	1.664
$r(T–O_1)$	1.892	1.853	1.879	1.859	1.804	1.834	1.824	1.843	1.789	1.664	1.764	1.804
$r(T–O_2)$	1.763	1.796	1.757	1.802	1.803	1.831	1.859	1.864	1.787	1.821	1.897	1.858
$r(Si_2–O_2)$	1.672	1.664	1.682	1.664	1.669	1.663	1.708	1.704	1.646	1.662	1.717	1.712
$<(C–O_1–T)$	107.0	109.7	101.9	109.7	87.9	89.6	98.3	119.0	–	–	–	–
$<(O_1–T–O_2)$	103.8	103.8	113.2	103.7	117.5	115.3	119.6	117.5	98.8	108.2	72.0	70.5
$<(Si_1–O_1–T)$	137.8	132.4	140.4	132.6	145.8	152.1	146.9	152.1	136.2	140.9	139.7	133.3
$<(T–O_2–Si_2)$	152.7	178.0	104.8	175.0	130.4	175.0	125.6	175.0	141.0	175.0	155.3	170.2
$<(H_1–O_2–T)$	–	–	–	–	–	–	116.7	125.9	–	–	104.9	108.6
$<(C–C_1–H_1)$	–	–	–	–	–	–	–	–	109.4	109.8	–	–

Table 2
Relevant geometric parameters obtained for reactants, transition states, Wheland complex and products using MNDO semiempirical method. The geometries correspond to *para* interaction. See Fig. 2 for labelling of geometrical parameters, and Fig. 5 for labelling of the species

Parameter	R_{adr1}		R_{adr2}		TS1		TS2		Whe		$<P_{adr}$	
T=	Al	Ga	Al	Ga	Al	Ga	Al	Ga	Al	Ga	Al	Ga
$r(C–O_1)$	1.412	1.404	1.412	1.405	2.291	2.231	1.512	1.522	4.074	4.331	5.202	5.297
$r(C–C_1)$	5.463	5.443	5.899	5.222	2.018	1.992	2.446	2.283	1.554	1.532	1.504	1.502
$r(C_1–H_1)$	1.095	1.102	1.092	1.104	1.098	1.104	4.297	4.204	1.129	1.132	–	–
$r(H_1–O_2)$	6.084	6.668	4.443	4.516	4.977	4.502	0.948	0.943	5.171	4.786	0.942	0.941
$r(Si_1–O_1)$	1.743	1.716	1.742	1.717	1.649	1.629	1.742	1.706	1.634	1.657	1.638	1.603
$r(T–O_1)$	1.558	1.919	1.564	1.918	1.462	1.782	1.481	1.808	1.443	1.804	1.402	1.668
$r(T–O_2)$	1.389	1.657	1.392	1.658	1.431	1.708	1.504	1.831	1.443	1.802	1.543	1.879
$r(Si_2–O_2)$	1.641	1.603	1.643	1.602	1.624	1.601	1.758	1.739	1.632	1.668	1.721	1.712
$<(C–O_1–T)$		122.9	122.0	124.8	122.3	115.6	114.7	68.6	119.2	–	–	–
$<(O_1–T–O_2)$		108.2106.3	108.3	106.3	108.4	106.6	108.2	107.9	108.7	105.1	105.2	101.0
$<(Si_1–O_1–T)$		112.4116.1	112.0	116.0	118.7	126.8	102.0	101.5	123.0	101.9	133.1	165.2
$<(T–O_2–Si_2)$		134.2166.7	134.3	166.9	126.0	148.3	125.4	128.2	123.0	102.2	120.4	125.0
$<(H_1–O_2–T)$	–	139.4	135.0	–	–	114.7	114.5	–	–	116.5	115.2	
$<(C–C_1–H_1)$	–	–	–	–	–	–	–	106.7	108.7	–	–	

control may exist, as it is the case of toluene alkylation by methanol [25], the orbital interactions between the reactants, which will be explained after, can play an important role for determining the *para/ortho*, selectivity, and this can depend on the zeolite framework composition.

When the stationary points localized as possible transition states were characterized, it was found that the values of the normal vibration modes of the stationary point gave one negative value characteristic of the transition states. In one case, a second negative value was found, but this is small and within the precision of the FORCE subroutine.

After the transition state, the Wheland intermediate is formed. This is a stable intermediate (Fig. 4 and Fig. 5), and its geometry (Tables 1 and 2) show that the methyl group has been completely transferred to the toluene, $r(C–C_1) = 1.50–1.55$ Å. The angle $CC_1H_1 = 109°$ shows the tetrahedral hybridization acquired by the C_1 atom. The H_1 atom remains bonded to the toluene with a distance, $r(C_1–H_1) = 1.1$ Å,

Table 3
Differences of enthalpies in the reaction of toluene alkylation by methanol (kcal/mol) calculated with PM3 and MNDO semiempirical methods

Method/ cluster [a]	ΔH_r [b]	ΔH_{ads1}	ΔH_{ads2}	ΔH_{act1}	ΔH_{act2}	ΔH_{whe}	ΔH_{des}
PM3							
ortho-Al	−18.36	−2.02	−4.76	78.88	79.64	−32.64	3.06
para-Al	−19.16	−1.82	−3.38	78.50	77.00	−34.45	2.90
ortho-Ga	−7.86	−6.78	−10.00	80.96	71.86	−27.82	7.90
para-Ga	−8.66	−6.76	−9.01	84.02	71.87	−32.94	8.97
MNDO							
ortho-B	−18.25	−1.97	−0.08	100.33	116.71	−34.86	0.31
para-B	−20.85	−2.28	−0.13	99.61	115.85	−36.68	0.37
ortho-Al	−16.79	−0.57	−0.36	105.82	110.35	−34.89	0.15
para-Al	−19.39	−2.06	−0.35	106.00	110.60	−36.52	0.08

[a] The cluster indicated is referred to the position of attack and the T atom.
[b] $\Delta H_r = (\Delta H(\text{zeo–H}) + \Delta H(\text{xylene})) - (\Delta H(\text{zeo–CH}_3) + \Delta H(\text{toluene}))$.

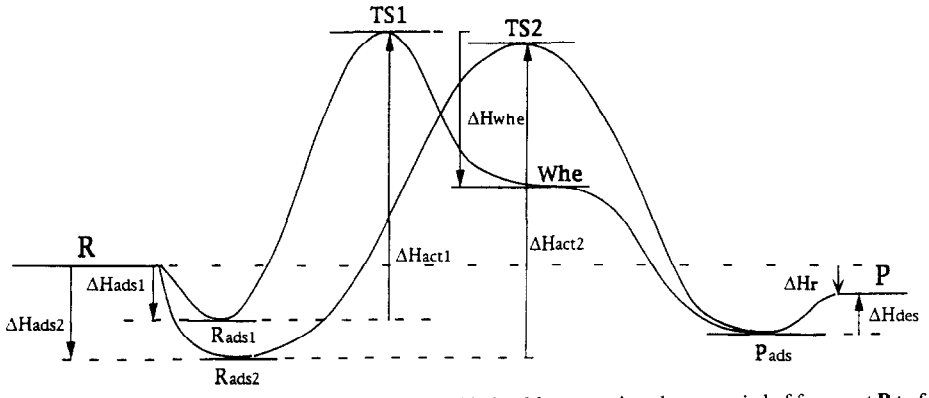

Fig. 5. Schematic depiction of the interactions between the occupied orbitals of fragment **A** and unoccupied of fragment **B** to form the complex **A–B**. The orbital controlling term is showed as ΔE_{ij}^{orb}, where i and j are the interacting orbitals. The energetic gap between molecular orbitals is showed as ΔE_{ij}.

slightly greater than the equilibrium one and out of the aromatic ring plane, as it corresponds to a classical Wheland intermediate. The stabilization of the complex is caused by the complete formation of the C–C_1 bond, which started to be formed in the transition state, as well as by the electrostatic interaction between the complex and the cluster of zeolite. The approximate charge of the complex is $+0.85\ e^-$ in PM3 calculations and $+0.99\ e^-$ in MNDO calculations. In both cases the results are within the range expected in a Wheland complex. In the case of MNDO, there is a larger charge separation between the complex and the cluster. The electronic distribution of the cluster shows a large charge in the basic oxygen O_2 ($-0.61\ e^-$), which is going to play an important role in the last step of the reaction.

Once the Wheland complex is formed, the *second step* of the reaction starts. It involves a transfer of the protonic hydrogen of the toluene to the cluster, in a step with no activation enthalpy and therefore very fast. This process has an ionic nature since there is a strong electrostatic interaction between the basic center of the cluster (O_2) and the protonic hydrogen of the toluene (H_1). In fact, the respective charges are $-0.7\ e^-$ and $+0.1\ e^-$, respectively. In this case, when the hydrogen, H_1, is slightly separated from the toluene, it is rapidly transferred to the cluster, with a constant decrease of the enthalpy along the reaction coordinate (Fig. 3). After this proton has been transferred, then the products of the reaction are formed.

4.2. Mechanism 2

In this case the adsorption process shows some peculiarity with respect to the former mechanism, that consist in the involvement of a different adsorption center in the cluster: the basic oxygen (O_2), which forms a bridging hydrogen bond with the H_1 of the toluene. The charge distribution obtained with PM3 method is more favorable to produce this interaction H_1–O_2 than that obtained with the MNDO. Moreover, that interaction is more favorable in Ga substituted zeolite than in Al substituted, since for the Ga containing cluster, the electronic density of the basic center, O_2, is greater than for the Al cluster. In the PM3 case, the magnitude of this interaction (ΔH_{ads2} in Table 3), is larger than that obtained in the first mechanism, because of the bridging hydrogen bond interaction observed in this second mechanism. There also exists a difference between the charge distribution in the O_2 atom being $-0.67\ e^-$ in PM3 and $-0.85\ e^-$ in MNDO, which explains the large differences in ΔH_{ads2} observed in the two methods. The optimized geometries (Tables 1 and 2) show the equilibrium distances of the interaction H_1–O_2, and the MNDO distance between those atoms is larger than in the PM3 case because of the weaker interaction in the MNDO case.

In mechanism 2 the transition state (TS2 in Fig. 4 and Fig. 5) contains some important differences regarding the former mechanism. The geometry obtained (Tables 1 and 2) shows that the methyl group is less transferred to the toluene (the $C–O_1$ distance is smaller and $C–C_1$ is greater than in the mechanism 1). Regarding the protonic hydrogen, it has been transferred to the zeolite cluster. The consequence of this is that the charge of toluene is very low ($+0.21\ e^-$ in PM3 and $-0.21\ e^-$ in MNDO). Therefore, in mechanism 2, the toluene molecule appears as acidic, and the cluster of the zeolite as basic. The cluster accepts the proton before transferring the CH_3 group. This mechanism takes place in one step, in a concerted way, and the intermediate is formed by a 6-atom ring, characteristic of other reactions of hydrocarbons over zeolites [26]. As a consequence, it requires two close active centers, the acidic and the basic. The calculations showed that when the reaction was forced to occur in the same center, strong stearic impediments between the methyl group and the toluene appeared with a big increment of the enthalpy of the system. This is a confirmation of the bicentric character of the reaction. Also, in this mechanism, the transition states in *ortho* and *para* are very similar in structure, charge distribution, and activation enthalpy. Another important aspect is that in the Ga cluster, the mechanism 2 is more favorable than mechanism 1 (ΔH_{act2}(Ga cluster) $< \Delta H_{act1}$(Ga cluster)), which means that the basic center in the Ga cluster plays a predominant role. The explanation for that is the charge on the basic oxygen next to the Ga atom ($-0.76\ e^-$), which is more negative in the Ga cluster than in the others. This is because of the higher bond polarity in the case of the Ga cluster concerning Al and B. In fact, this mechanism starts with a hydrogen bonding interaction between the hydrogen atom of the toluene and the basic oxygen of the zeolite. The geometry obtained after this adsorption process, which is stronger than that of the first mechanism, facilitates the interaction between the carbon atom of the toluene and the carbon atom of the alkylating agent ($C–C_1$ interaction, see Fig. 1), which is a weaker interaction. The concerted transition state supports the reliability of this mechanism, as correspond to many reactions over zeolites. The basicity of the oxygen atom plays an important role in this mechanism of bifunctional catalysis.

After the transition state, the products of reaction were quickly formed. The geometry of the adsorbed xylenes is similar to mechanism 1. The desorption energies are also small, and the distance between the xylene and the cluster of zeolite is large as corresponds to Van der Waals complex. Although the calculations support this mechanism, there is some concern from the chemical point of view since it involves the toluene acting as a Brønsted acid with respect to the basic centers of the zeolite.

4.3. The role of the covalent interactions in Mechanism 1

Although the electrophilic alkylation in liquid phase proceeds trough free carbocation, the behavior in zeolites is different. Up to now, free carbocations can hardly be distinguished in zeolites [27] because the existence of easy electron flow from the cation to the framework. The adsorption process supports this effect, and after that, when the organic molecule closely approaches the zeolite, an electronic transference between the adsorbed cation and the organic molecule can easily occur. This is the case in the toluene alkylation by methanol over zeolites. The methyl cation is adsorbed in the zeolite in the form modelized in the calculations, forming a methoxy group through the interaction with an oxygen atom, in this case the bridged SiOAl. Thus, the approach of the toluene to the alkylating agent produces an electronic transference from the toluene to the zeolite. This transference can be understood by means of perturbation theory applied to reactivity.

According to the perturbation theory of reactivity [28], the change in energy of a system initially formed by the reactants **A**, and **B** to form the complex **A–B** can be represented by the following equation [29]:

$$\Delta E^{(Pert)} = \sum_{k<1} \frac{Qk\,Ql}{R_{kl}} - 2\cdot\sum_{a,b}\Big(\sum_{r}^{oc}(C_r^a)^2 + \sum_{s}^{oc}(C_s^b)^2\Big)\beta_{ab}\cdot S_{ab} + \Big(\sum_{r}^{oc}\sum_{s}^{virt} - \sum_{s}^{oc}\sum_{r}^{virt}\Big)^2 \frac{\big(\sum_{a,b} C_4^a C_s^b \beta_{ab}\big)^2}{E_r - E_s} \qquad (1)$$

The first term corresponds to the pure ionic interactions between the two molecules and is usually the most energetic contribution. The second term corresponds to a destabilizing factor due to the energetic repulsion between the occupied orbitals of the two molecules. Finally, the last term corresponds to the stabilizing interaction between the occupied and unoccupied orbital of the molecules, the most important being the HOMO–LUMO interactions (Fig. 5). Considering that the perturbation is small in the transition state of the first mechanism, TS1, the PM3 optimized geometry served to perform a perturbed molecular orbital (PMO) analysis of the system at the ab initio HF/STO-3G level. In this transition state, the covalent interactions are important, and this can be deduced by seeing the charge distribution of the methyl group. An electronic transference between the zeolite and the toluene is taking place, and the C–O_1 and C–C_1 bonds are simultaneously breaking and forming. In this case of electrophilic substitution, the ionic interactions play the same role in alkylating the positions *ortho* and *para* because the charge distribution is the same in the two positions of the toluene. With regard to the role of covalent interactions, they can be important if the occupied–unoccupied orbital interaction term in the Eq. 1 increases. This interaction can be calculated by means of the PMO analysis. The two fragments whose interaction is calculated are the alkylating agent and the toluene. The electronic donor will be the toluene and the electronic acceptor will be the zeolite. The calculations have been performed for the Al-substituted cluster in the *para* and *ortho* positions of attack. From the results showed (Table 4), the initial HOMO–LUMO gap is lower in the case of the *para* interaction. This is important because little energetic difference between the molecular orbitals means increasing stabilization effect in Eq. 1. In addition, the frontier orbital density, C_r^a, in Eq. 2, is higher in the *para* interaction respect to the *ortho*. The final result of the calculations show a higher stabilization effect in the case of the *para* attack, which means that this isomer can be obtained more easily. From the results of those calculations, three conclusions can be obtained. The first conclusion is that only HOMO–LUMO interactions are important. This is in agreement with the frontier orbital theory of Fukui [30]. Second, the energy of these covalent interactions is high (48.6 and 38.3 kcal/mol), so they can play an important role in catalysis when ionic effects are very similar to distinguish changes in selectivity in process in which the first order term, the ionic factor, is sim-

Table 4
Perturbed molecular orbital (PMO) analysis of the transition state of the first mechanism, TS1 (Fig. 4)

Property	*para*-Interaction	*ortho*-Interaction
HOMO(tol)–LUMO(alk. agent) gap (eV)	8.87	9.14
$C_{tol}^{(HOMO)}$ (frontier orbital density)	0.54	0.47
$C_{alk.\ agent}^{(LUMO)}$ (frontier orbital density)	0.89	0.89
HOMO(tol)–LUMO(alk. agent) overlap	0.11	0.10
HOMO(tol)–LUMO(alk. agent) orbital interaction (kcal/mol)	48.6	38.3
HOMO(tol) electronic population	1.77	1.82
LUMO(alk. agent) electronic population	0.40	0.46

The fixed geometry of the system has been obtained from the previous PM3 calculations (Table 1). The analysis corresponds to the Al-substituted cluster, and the *para* and *ortho* interaction with toluene.

ilar in two or more positions of attack. Third, the frontier orbital interactions are more important in the case of the *para* attack because the interaction is greater in this position (48.6 kcal/mol compared with 38.3 kcal/mol in *ortho*). This last conclusion is important in catalysis in order to explain *para*/*ortho* selectivities experimentally observed in aromatic alkylation over large pore zeolites [27]. The PMO analysis show another two important results, the overlapping HOMO(tol)–LUMO(alk. agent) which is little as correspond to small perturbations of the system, and the frontier orbital population which is lower than 2.0 in the HOMO(tol) and higher than 0.0 in the LUMO(alk. agent), which means that an electronic transfer from the HOMO to the LUMO is taking place (Table 4).

5. Conclusions

Two reaction mechanisms have been found in the molecular orbital calculations of the alkylation reaction of toluene on zeolite clusters. In these mechanisms we have localized the different intermediate species and transition states. The first mechanism is analogous to the classical two-step aromatic alkylation, passing through a Wheland intermediate. The second is a concerted one-step mechanism.

In the first mechanism, after de adsorption localized on the C–C_1 atoms, the transition state is characterized by the transference of the methyl group to the toluene. The geometry of this transition state shows distances and angles according to the precursor of the Wheland intermediate. After the transition state, the Wheland intermediate is formed, with analogous geometry to the classical mechanism, and finally, the proton of the toluene is transferred to an oxygen atom of the zeolite cluster.

The second mechanism begins with a different adsorption mechanism in which not only the C–C_1 atoms participate, but also the H_1–O_2 atoms. The transition state is characterized by a strong H_1–O_2 interaction. The transference of the methyl group is simultaneous to the transference of the proton, in a one-step concerted mechanism. The possibility of this second mechanism suggests that the basic oxygen centers of zeolite could be important for its reactivity and must be taken into account to explain reactions like hydride abstraction. This mechanism correspond to acid catalysis because need the Brønsted acid site to form the alkylating agent. The role of hydrogen bonding interaction is remarked as a starting point of the reaction, being the products the same as in first mechanism.

The role of the covalent interactions in the first mechanism has been studied by perturbed molecular orbital (PMO) analysis, showing the existence of strong interactions between occupied–unoccupied molecular orbitals. In this case, the toluene acts as an electronic donor through its HOMO, and the alkylating agent as the electronic acceptor through its LUMO. The energy of these covalent interactions, mainly HOMO–LUMO, which is higher for the *para* position respect to the *ortho*, could help to explain the *para* selectivity observed in toluene alkylation when the importance of the covalent interactions increase by increasing the Si/Al ratio of the catalyst, or by changing B by Ga and Al, i.e. when increasing the softness of the zeolite.

Acknowledgements

Financial support of CICYT (MAT 94-0359-C02-01) and Ministerio de Educación y Ciencia of Spain are gratefully acknowledged. The support of Centro Informático and Departamento de Química Física of the University of Valencia for the use of their computing facilities are also acknowledged.

References

[1] (a) A. Corma, Stud. Surf. Sci. Catal., 49 (1989) 49; (b) J.A. Rabo and G.J. Gajda, Catal. Rev. Sci. Eng., 31 (4) (1989–90) 385.

[2] L.A. Pine, P.J. Maher and W.A. Watcher, J. Catal., 85 (1984) 466.
[3] (a) D. Barthomeuf, Mater. Chem. Phys., 17 (1987) 49; (b) A.G. Pelmenshchikov, E.A. Paukshtis, V.G. Stepanov, V.I. Pavlov, E.N. Yurchenko, K.G. Ione, K.G. Zhidomirov and S. Beran, J. Phys. Chem., 93 (1989) 6725; (c) J. Sauer, H. Horn, M. Haeser and R. Ahlrichs, Chem. Phys. Lett., 173 (1990) 26; (d) J. Dwyer, in E.G. Derouane et al. (Eds.), Zeolites Microporous Solids: Synthesis, Structure, and Reactivity, Kluwer, Dordrecht, 1992, p. 303; (e) B.G. Baekelandt, W.J. Mortier, J.L. Lievens and R.A. Schooneheydt, J. Am. Chem. Soc., 113 (1991) 6730; (f) J. Lintrakul and S. Hannongbua, J. Mol. Struct. (Theochem), 280 (1993) 139.
[4] D.A. Keyworth, J. Nieman, P. O'Connor and Ch.W. Stanger, NPRA Annual Meeting, March 1987, San Antonio, TX, AM-87-62.
[5] N.Y. Chen and W.E. Garwood, J. Catal., 52 (1978) 453.
[6] (a) S. Namba, H. Ohta, J.H. Kim and T. Yashima, 75 (1993) 1685; (b) S.G.T. Bhat, J. Catal., 75 (1982) 196.
[7] Bhat, S.G.T. Halgeri, A.B. and Prasada Rao, T.S.R. Ind. Eng. Chem. Res., 28 (1989) 890.
[8] (a) Cavallaro, S. Pino, L. Tsiakaras, P. Giordano, N. and Rao, B.S.S. Zeolites, 7 (1987) 408; (b) Corma, A. Sastre, G. Viruela, R. and Zicovich-Wilson, C. J. Catal., 136 (1992) 521; (c) Oh, S.H. and Lee, W.Y. Stud. Surf. Sci. Catal., 75 (1993) 1685.
[9] J. Rakoczy and T. Romotowski, Zeolites, 13 (1993) 256.
[10] G. Mirth and J. Lercher, J. Catal., 132 (1991) 244.
[11] M.J.S. Dewar and W. Thiel, J. Am. Chem. Soc., 99 (1977) 4899.
[12] J.J.P. Stewart, J. Comp. Chem., 10 (1989) 209.
[13] J.J.P. Stewart, MOPAC, A general molecular orbital package, Version 6.0, Vol. 10, QCPE, 1990, p. 455.
[14] (a) C.G. Broyden, J. Inst. Math. Appl., 6 (1970) 222; (b) R. Fletcher, Comp. J., 13 (1970) 317; (c) D. Goldfarb, Math. Comp., 24 (1970) 23; (d) D.F. Shanno, J. Opt. Theor. Appl., 46 (1) (1985); (e) D.F. Shanno, Math. Comp., 24 (1970) 647.
[15] J.N. Murrell and K.J. Laidler, Trans. Faraday Soc., 64 (1968) 371.
[16] J.J.P. Stewart, J. Comp. Chem., 10 (1989) 221.
[17] V.I. Minkin, B.Ya. Simkin and R.M. Minyaev, Quantum Chemistry of Organic Compounds. Mechanisms of the Reactions, Springer-Verlag, 1990, p. 74.
[18] (a) W.J. Hehre, R.F. Stewart and J.A. Pople, J. Chem. Phys., 51 (1969) 2657; (b) W.J. Hehre, R. Ditchfield, R.F. Stewart and J.A. Pople, J. Chem. Phys., 64 (1970) 5142.
[19] M.R. Peterson and R.A. Poirier, MONSTERGAUSS, Department of Chemistry, Toronto University, Ontario M55 1A1, Canada.
[20] A. Corma, C. Zicovich and P. Viruela, J. Phys. Chem., 99 (1995) 13244.
[21] (a) V.B. Kazansky, Acc. Chem. Res., 24 (1991) 379; (b) G. Mirth, A. Kogelbauer and J.A. Lercher, Proceedings of the 9th International Zeolite Conference, Montreal, 1992; (c) A.G. Pelmenschikov, G. Morosi and A. Gamba, Proceedings of the 9th International Zeolite Conference, Montreal, 1992, p. 537.
[22] P. Viruela, C. Zicovich-Wilson and A. Corma, J. Phys. Chem., 93 (1993) 13713.
[23] (a) K.J. Chon, J.C. Lin, Y. Wang and G.H. Lee, Zeolites, 6 (1986) 35; (b) J.L. Schlenker, T.J. Pluth and J.V. Smith, Mater. Res. Bull., 14 (1979) 849; (c) D.H. Olson and E. Dempsey, J. Catal., 13 (1969) 221.
[24] A. Corma, in D. Barthomeuf et al. (Eds.), Guidelines for Mastering the Properties of Molecular Sieves, Plenum Press, New York, 1990, p. 299.
[25] A. Corma, F. Llopis, P. Viruela and C. Zicovich-Wilson, J. Am. Chem. Soc., 116 (1994) 134.
[26] I.N. Senchenya and V.B. Kazansky, Catal. Lett., 8 (1991) 317.
[27] J.A. Rabo and G.J. Gajda, Catal. Rev. Sci. Eng., 31 (4) (1990) 385.
[28] M.H. Whangbo, H.B. Schlegel and S. Wolfe, J. Am. Chem. Soc., 99 (1977) 1296.
[29] (a) G. Klopman and R.F. Hudson, Theor. Chim. Acta, 8 (1967) 165; (b) G. Klopman, J. Am. Chem. Soc., 90 (1968) 223.
[30] K, Fukui, Angew. Chem., Int. Ed. Engl., 21 (1982) 801.